scientific reports

Check for updates

OPEN

Efficient PEGylated magnetic nanoniosomes for co-delivery of artemisinin and metformin: a new frontier in chemotherapeutic efficacy and cancer therapy

Rasoul Shahbazi[1], Zohreh Mirjafary[1]✉, Nosratollah Zarghami[2]✉ & Hamid Saeidian[3]

Two strategies were employed to modify the performance of the nano-niosome drug delivery system. Initially, the surface of the nano-niosomes underwent modification through the inclusion of polyethylene glycol, thereby altering its properties. Additionally, the core of the nano-niosomes was equipped with Fe_3O_4 magnetic nanoparticles to impart magnetic characteristics to the system. This study presents the development of PEGylated magnetic nanoniosomes (PMNios) for the co-delivery of artemisinin (ART) and metformin (MET) in cancer therapy, highlighting significant advancements in chemotherapeutic efficacy. The magnetization of the nano-niosomes facilitated the targeted delivery of drugs to specific tissues, while PEGylation improved the bioavailability of the nano-niosomes. These PEGylated magnetic niosomes (PMNios) were then loaded with artemisinin and metformin drugs. The synthesized PMNios were thoroughly evaluated in terms of zeta potential, size, morphology, and entrapment efficiency. The PMNios achieved a drug loading efficiency of 88%. They exhibited an average size of 298 nm, a polydispersity index of 0.32, and a zeta potential of − 19 mV, indicating the complete stability. SEM and TEM images of the PMNios revealed a spherical morphology. Subsequently, the PMNios were compared with other forms of nano-niosomes, including empty niosomes, non-magnetic niosomes, and non-PEGylated niosomes. The encapsulation of the nano-niosomes with magnetic nanoparticles allows for faster delivery of the encapsulated drugs to the tumor site, while PEGylation improved the stability, bioavailability, and controlled release of the PMNios. Furthermore, the in-vitro effectiveness of various formulations of the PMNios against A549, a lung cancer cell line, demonstrated that the PMNios exhibited appropriate toxicity towards cancer cell lines in the presence of an external magnetic field. Gene expression level of Bcl2 were lower for the PMNios-ART-MET system, whereas the level of *Bax* were higher than the other group. The PMNios-ART-MET system also demonstrated well internalization into the A549 cells and preponderant endocytosis. These findings underscore the novelty and potential of PMNios as a robust platform for the targeted co-delivery of hydrophilic and hydrophobic drugs, promising a new frontier in cancer therapy by enhancing the therapeutic index and minimizing side effects.

Keywords Magnetic noisome, Metformin, Artemisinin, Lung cancer, Targeted drug delivery system

Niosomes have emerged as innovative drug delivery systems composed of nonionic surfactant vesicles, offering exceptional properties for delivering both hydrophilic and hydrophobic drugs[1,2]. These nano-carriers have gained popularity due to their uniform and straightforward synthesis, extended shelf-life, cost-effectiveness, biocompatibility, chemical and physical stability, and low toxicity. Nano-niosomes have found applications in various fields such as cancer therapy, skin care treatments, gene delivery, drug targeting, and anti-neoplastic treatment. One notable application of niosomes is their use in targeted co-delivery of multiple drugs to specific tissues[3,4]. Among the different methods developed for targeting cancerous tissues, magnetic drug delivery

[1]Department of Chemistry, Science and Research Branch, Islamic Azad University, Tehran, Iran. [2]Department of Medical Biotechnology, Faculty of Advanced Medical Science, Tabriz University of Medical Sciences, Tabriz, Iran. [3]Department of Science, Payame Noor University (PNU), P.O. Box 19395-3697, Tehran, Iran. ✉email: zmirjafary@srbiau.ac.ir; zarghami@tbzmed.ac.ir

systems have gained attention. Magnetic niosomes, a relatively unexplored nano-carriers, involve the using of magnetized nanoparticles as targeting factors. By applying an external magnetic field, these magnetic nano-carriers can be guided to the desired tumor sites, leading to enhanced drug condensation and improved overall efficiency of the drug co-delivery system[5–8].

The performance of niosome drug co-delivery systems can be enhanced by employing a different approach, which involves coating the surface of nano-niosomes with hydrophilic polymers such as polyethylene glycol (PEG). This coating serves to improve the bioavailability of the niosomes. PEG possesses several desirable properties, including being non-antigenic, non-immunogenic, non-toxic, and highly water-soluble. Moreover, it extends the blood circulation time of the niosomes by preventing enzymatic degradation. The exceptional hydrophilicity of PEG has been found to be responsible for its ability to absorb water on the surface of nano-niosomes. Consequently, this hinders the recognition and removal of the nano-niosomes by macrophages[9–12]. Ultimately, the modification of the niosome surface allows the nano-niosomes to remain in the body for a longer period, giving them more time to locate their target tissue before being eliminated by macrophages. In this study, we present our findings on the surface modification of nano-niosomes using both magnetization and PEGylation techniques (Fig. 1)[13–15].

The effect of magnetization and PEGylation on nano-niosomes has been conducted in previous studies[16–19]. To assess this innovative system, the anti-cancer efficiency of artemisinin (ART) and metformin (MET) were examined. Initially, magnetic Fe_3O_4 nanoparticles were synthesized and incorporated into the nano-niosomes to create a magnetic drug delivery system. The doses of ART and MET were selected based on extensive literature review and preliminary experimental data aimed at identifying concentrations that provide optimal therapeutic efficacy while minimizing toxicity. ART doses ranging from 10 to 100 μM have been reported to exhibit significant anticancer activity. Through preliminary cytotoxicity assays on A549 lung cancer cells, a dose of 50 μM was chosen as it maximized anticancer effects without excessive toxicity. MET doses between 1 and 10 mM have shown effective anti-proliferative properties in various studies. We selected a dose of 5 mM for MET, based on preliminary experiments that indicated this concentration synergized effectively with ART and provided substantial anticancer activity[20–23]. Additionally, PEGylated niosomes were prepared using Sorbitan monostearate (Span 60) and Cholesterol. The PEGylated magnetic nano-niosomes (hereinafter referred to as "PMNios") were then analyzed for their size, entrapment efficiency (EE), polydispersity index (PDI), zeta potential, and morphology. Subsequently, the impact of the PMNios bearing ART and MET drugs on A549 lung cancer cells was evaluated in the presence or absence of an external magnetic field. Various lung cell lines, including both healthy and cancerous cells, were utilized as cell-based models to assess the effects of the PMNios (Fig. 1)[24]. According to previous studies, ART prevented tumor growth in 4T1 tumor-bearing mice and prevented their death. CTLs and CD4 + IFN-γ + T cells remarkably increased while Treg and MDSC frequencies remarkably decreased in the 4T1 tumor-bearing mice after treatment with ART. ART phytochemical drugs

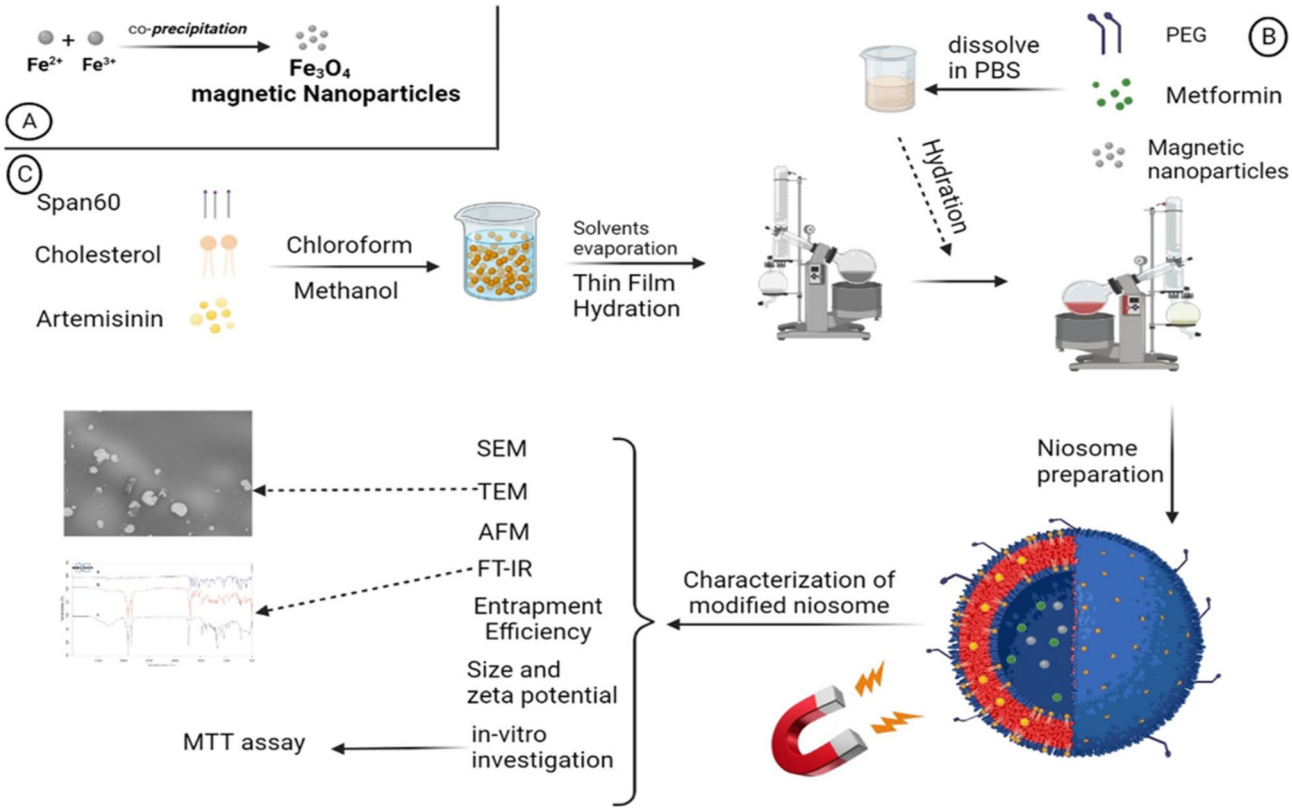

Fig. 1. Schematic synthesis procedure of the PMNios-ART-MET.

prevented 4T1 tumor expansion in vivo by cultivating T cell activation and suppression of the immune system from MDSCs cells and Tregs cells in the tumor[24].

Materials and methods

Chemicals

Iron (II) chloride tetrahydrate ($FeCl_2 .4H_2O$), iron (III) chloride hexahydrate ($FeCl_3 .6H_2O$), polyethylene glycol 4000 (PEG 4000), sorbitan monostearate (Span60), cholesterol, phosphate-buffered saline (PBS), chloroform, and methanol were obtained from Sigma, USA. A549 cells were obtained from the Tabriz University of Medical Sciences (Faculty of Advanced Medical Sciences). Dialysis tubing (cellulose membrane avg. flat width 1 cm and molecular weight cut-off 14,000 Da) were obtained from Sigma, USA. Metformin hydrochloride and artemisinin were obtained from Sigma, USA.

Synthesis of Fe_3O_4 nanoparticles

The synthesis of magnetic Fe_3O_4 nanoparticles (MNPs) was carried out using the co-precipitation technique under alkaline conditions[16]. To prepare the nanoparticles, 3.7 g (18.6 mmol) of $FeCl_2 .4H_2O$ and 6.36 g (23.5 mmol) of $FeCl_3 .6H_2O$ were separately dissolved in 75 mL of deionized water in a round bottom flask, under an N_2 atmosphere with continuous stirring. The resulting solution was then stirred at 80 °C under N_2 atmosphere for 2 h. Subsequently, 15 mL of NH_4OH was added dropwise to the solution under N_2 atmosphere for an additional 2 h. After allowing the suspension to cool down to room temperature, the black sediments were collected and subjected to multiple washes with ethanol and deionized water. Finally, the black precipitates were dried in an oven at 60–70 °C for 4 h. The analysis of the Fe_3O_4 nanoparticles was conducted using X-ray diffraction (XRD) with the Tongda TD-3700 instrument. To identify the chemical bonds present in the synthesized nanoparticles, a Fourier transform spectrometer (Tensor, Bruker) was utilized at 25 °C. The magnetic properties of the nanoparticles were investigated using a vibrating-sample magnetometer (VSM) with the MDKB model (Danesh Pajouh Company).

Synthesis of the PEGylated magnetic nano-niosomes (PMNios)

Niosomes were prepared using the thin film hydration method[17]. Initially, a mixture of cholesterol, Span 60, and the hydrophobic ART drug was dissolved in a mixture of 6 mL methanol and 3 mL chloroform. The molar ratio of these components was 1:9:1, respectively, and the final solution volume was 10 mL. The solvent was then evaporated using a vacuum rotary evaporator at 60 °C. This process resulted in the formation of a thin film in the round-bottom-flask. Subsequently, a thin layer of pro-niosome was hydrated by adding 10 mL of phosphate-buffered saline (PBS) solution with a pH of 7.4. In this step, 0.01 mmol of MET and 0.01 mmol of PEG were dissolved in the PBS solution, and 0.01 mmol of synthesized magnetic nanoparticles were added to the same solution. The mixture was then transferred to a rotary evaporator and subjected to a temperature of 60 °C for 30 min (Fig. 1). Afterward, the solution was sonicated in an ice bath for 10 min to form small unilamellar niosomes, while preventing niosome leakage[25]). To remove any un-entrapped ART and MET and magnetic nanoparticles, the solution was centrifuged at 14,000 relative centrifugal force (rcf) for 50 min. at 4 °C. Finally, the PMNios-ART-MET formulation was obtained by passing the solution through 0.4- and 0.2-µm pore sizes syringe filters twice (Sartorius AG, Germany). Various modified noisome formulations were prepared with the mentioned methods (Table 1).

The investigation of synthesized nano-niosomes (Table 1) involved the examination of their size, morphology, zeta potential, and polydispersity index (PDI). The dynamic light scattering (DLS) technique using the Malvern Zeta Sizer (Malvern Instrument, Malvern, UK) was employed to assess the PDI, zeta potential, and average dispensation sizes of nano-niosomes[26]. Each test was conducted in triplicate, with the nano-niosomes diluted in a ratio of 100:1 with deionized water. The morphology and size of the synthesized niosomes were estimated using Transmission Electron Microscope (TEM, Zeiss EM900, Oberkochen, Germany), Field Emission Scanning

Name	S/C rate	ART	MET	PEG	Size (nm)	PDI	ZP (mv)	EE% -MNPs	EE% drug
Blank-Nios	9:1	–	–	–	185 ± 1	0.25 ± 0.01	− 21 ± 0.5	–	–
PEG-Nios	9:1	–	–	1	215 ± 1	0.20 ± 0.01	− 16 ± 0.5	–	–
Nios-ART	9:1	1	–	–	260 ± 1	0.28 ± 0.01	− 20 ± 0.5	–	88
Nios-MET	9:1	–	1	–	255 ± 1	0.27 ± 0.01	− 22 ± 0.5	–	83
MNP-Nios-ART	9:1	1	–	–	265 ± 1	0.29 ± 0.01	− 22 ± 0.5	91	85
MNPs-Nios-MET	9:1	–	1	–	261 ± 1	0.28 ± 0.01	− 23 ± 0.5	89	80
PEG-Nios-ART	9:1	1	–	1	267 ± 1	0.26 ± 0.01	− 18 ± 0.5	–	90
PEG-Nios-MET	9:1	–	1	1	262 ± 1	0.29 ± 0.01	− 20 ± 0.5	–	87
PMNios-ART	9:1	1	–	1	295 ± 1	0.30 ± 0.01	− 17 ± 0.5	90	84
PMNios-MET	9:1	–	1	1	275 ± 1	0.29 ± 0.01	− 19 ± 0.5	88	80
PMNios-ART-MET	9:1	1	1	1	298 ± 1	0.32 ± 0.01	− 19 ± 0.5	90	85

Table 1. Characterization of various modified noisome. S: Span60, C: cholesterol, ZP: zeta potential (mV), PDI: polydispersity index, EE: entrapment efficiency, MNPs: magnetic nanoparticles, Nios: noisomes, ART: artemisinin, MET: metformin, PEG: polyethylene glycol, PMNios: PEGylated magnetic nano-niosomes.

Electron Microscopy (FE-SEM, Tescan MIRA3 FEG-SEM, Czech), and atomic force microscopy (AFM, Ara-AFM 0101 A, Iran). Additionally, the XRD pattern of the niosomes was determined using X-ray diffraction (XRD) with the Tongda TD-3700 instrument[27–30]. The long-term stability of the particles was assessed, after two months of storage at 4 ± 1 °C. The selection of 4 °C as the primary storage temperature was based on standard nanoparticle storage practices, which aim to minimize kinetic energy, thereby reducing the risk of aggregation and degradation. Preliminary studies indicated that PMNios maintained their physicochemical properties more effectively at 4 °C, with minimal changes in size, PDI, and zeta potential, compared to storage at 25 °C, where increased instability was observed.

Entrapment efficiency of the niosomes

The determination of the encapsulation efficiency (EE%) of ART-MET-loaded PMNios was conducted using *o*-phenylenediamine compound. To begin, the PMNios-ART-MET formulation was subjected to centrifugation at 15,000 rpm for 15 min. Following this, 100 µL of the supernatant was mixed with 100 µL of *o*-phenylenediamine (1.5 g/L in DMF) and 100 µL of the PBS solution. The mixture was then heated at 80 °C for 25 min, resulting in a light green-blue colored liquid. This liquid was subsequently cooled to room temperature, and 1 mL of DMF was added to the solution. The concentration of ART and MET was determined by measuring the absorption at 205 nm and 233 nm, respectively using ultraviolet-visible spectroscopy[31]. The ratio of encapsulated ART and MET was calculated by subtracting the amount of free ART/MET in the supernatant from the initial amount added in the PMNios-ART-MET formulation. The EE% was estimated using the following equation:

$$\mathrm{EE}\ (\%)\ =\ [(\mathrm{C_t}-\ \mathrm{C_f})\ /\mathrm{C_t}]\ \times\ 100$$

Where C_t is the concentration of total drug and C_f is the concentration of free drug in the supernatant. Values are reported as an average for three experiments ± SD.

In this study, each noisome formulation (Table 1) was diluted with methanol in a ratio of 1–25 mL. The optical density of the resulting solution was then measured at two specific wavelengths, namely 205 nm and 233 nm. These wavelengths correspond to the maximum absorption peaks of ART and MET, respectively[22,23]. Methanol was employed to disrupt the niosome structure, facilitating the release of ART and MET.

Evaluation of the in-vitro drugs release from the PMNios

The PMNios solution was filled into a dialysis tube, which had a cellulose membrane with an average flat width of 10 mm and a molecular weight cut-off of 14,000 Da. Subsequently, the samples were transferred into a graduated cylinder containing 20 mL of the PBS solution with a pH of 7.4. The system was then stirred and incubated at 37 °C. At specific time intervals, 1 mL of the sample was collected and analyzed by measuring the absorbance at 205 nm and 233 nm. The results are reported as an average for three experiments ± SD.

Bioavailability of artemisinin and metformin

The basic limits of the utilization of ART as a suitable anti-cancer drug comes from poor solubility, short half-life and poor bioavailability when used in pure form. The low solubility of pure ART in an aqueous medium usually dictates its low absorption and low bioavailability at various prescribes. Also, it is possible to interact with other natural bioactive compositions. The efficacy and bioavailability of ART can be improved by the novel drug delivery system like as modified niosome in combination with other anticancer drugs like as MET. The net bioavailability of ART and MET after intravenous and oral prescription was 12.3% and 55% respectively. By encapsulation of ART and MET in PEGylate niosome the rate of bioavailability was improved. PEGylate niosomes in the circulatory system were broken down and both encapsulated drugs were released gradually. This process improves the low bioavailability of ART and MET.

MTT cytotoxicity studies

The cytotoxic efficacy of various modified noisome formulations (Table 1) on A549 cancer cell line and human epithelial (HBE) cells was evaluated by MTT assay. For the MTT assay, both positive and negative controls were included. The negative control consisted of a solvent buffer along with untreated cells and MTT[32,33]. The positive control involved the use of MTT reagent, untreated cells, and DMSO. Additionally, a blank sample was prepared using MTT reagent, untreated cells, and empty modified niosomes. Finally, the cytotoxicity (expressed as a percentage) of the tested formulations (Table 1) against the A549 cancer cell line was evaluated using the following formulation:

$$\mathrm{C}\ \%\ =\ [(1\ -\ \mathrm{A_n})\ /\ \mathrm{A_c}]\ \times\ 100$$

Where C is the toxicity percentage, A_n and A_c are the amounts of absorbance of the niosome and control-treated wells. Amounts are represented as the average for three experiments ± SD.

Cell uptake

FITC-labeled nanoparticles (PMNios-MET, PMNios-ART, and PMNios-ART-MET) were incubated with A549 cells at a concentration of 15 µM for 1, 4, and 8 h. Following incubation, cells were washed twice with PBS and subsequently stained with DAPI for 15 min to visualize nuclei. Cellular uptake of nanoparticles was assessed using a Leica TCS SPE confocal laser scanning microscope. FITC fluorescence was detected with an excitation wavelength of 495 nm and an emission wavelength of 519 nm.

Statistical analysis

One-way ANOVA test was applied for the statistical analysis of various tests[25]. To evaluate the ANOVA test, a posterior Bonferroni t-test was represented. A p-value (* $p<0.05$, ** $p<0.01$, *** $p<0.001$) was considered meaningful. All values are presented as the average ± SD.

Results and discussion

Physicochemical properties of the PMNios-ART-MET

Physicochemical characterization of the PMNios-ART-MET through XRD (Fig. 2a), VMS (Fig. 2b), TEM (Fig. 2c) FT-IR (Fig. 3) was analyses in terms of morphology, size, ferromagnetism properties and accuracy of drugs encapsulation. XRD analysis indicated that the nanoparticles exhibit a structure associated with the Fe_3O_4 phase, and the size of certain nanoparticles falls within the range of 10–17 nm (Fig. 2a). TEM analysis confirmed that the Fe_3O_4 nanoparticles have a uniform morphology, as depicted in Fig. 2b. These nanoparticles possess a spherical morphology. Further the VSM magnetization curve (Fig. 2c), exhibited distinct characteristics of either ferromagnetism or superparamagnetic. Notably, this curve did not exhibit any coercivity, remanence, or hysteresis. Based on the VSM curve, the saturation magnetization of the Fe_3O_4 nanoparticles was determined to be 68 emu/g. Although the nanoniosomes construction influences the synthesized nanoparticle size and PDI, all the synthesized niosomal formulations were small in particle size and PDI (< 250 nm) along with monodisperse features. This feature allows the compatibility of the thin film hydration method for industrial-scale and clinical use of these nanoparticles with excellent reproducibility. On the other hand, the PEGylation of niosome leads to prevent agglomeration and clomping of niosome and followed by makes this Nano-carrier a suitable case for industrial-scale and clinical use. Also, none of the niosome composition materials have a cytotoxicity effect on normal cells, then this Nano-carrier is an acceptable case for clinical use.

The presence of ART and MET in the PMNios was confirmed through FT-IR analysis (Fig. 3). The Span 60 spectrum exhibited distinct peaks at 3450/cm, indicating O–H stretching, and in the range of 2830–2950/cm,

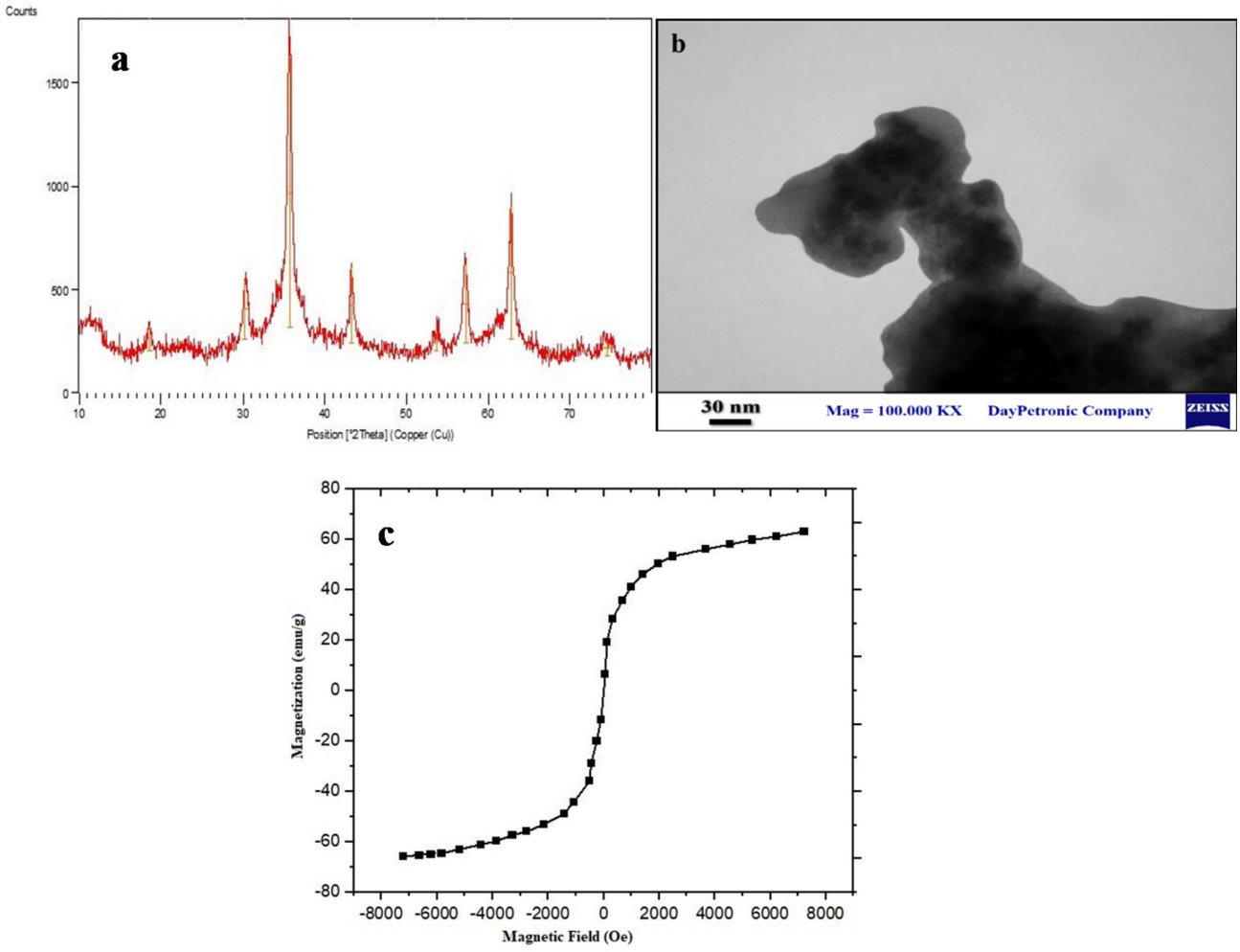

Fig. 2. (a) X-ray diffraction (XRD) patterns of the PMNios-ART-MET; (b) the transmission electron microscopy of the synthesized Fe_3O_4 nanoparticles; (c) Vibrating-sample magnetometer curve of the Fe_3O_4 nanoparticles.

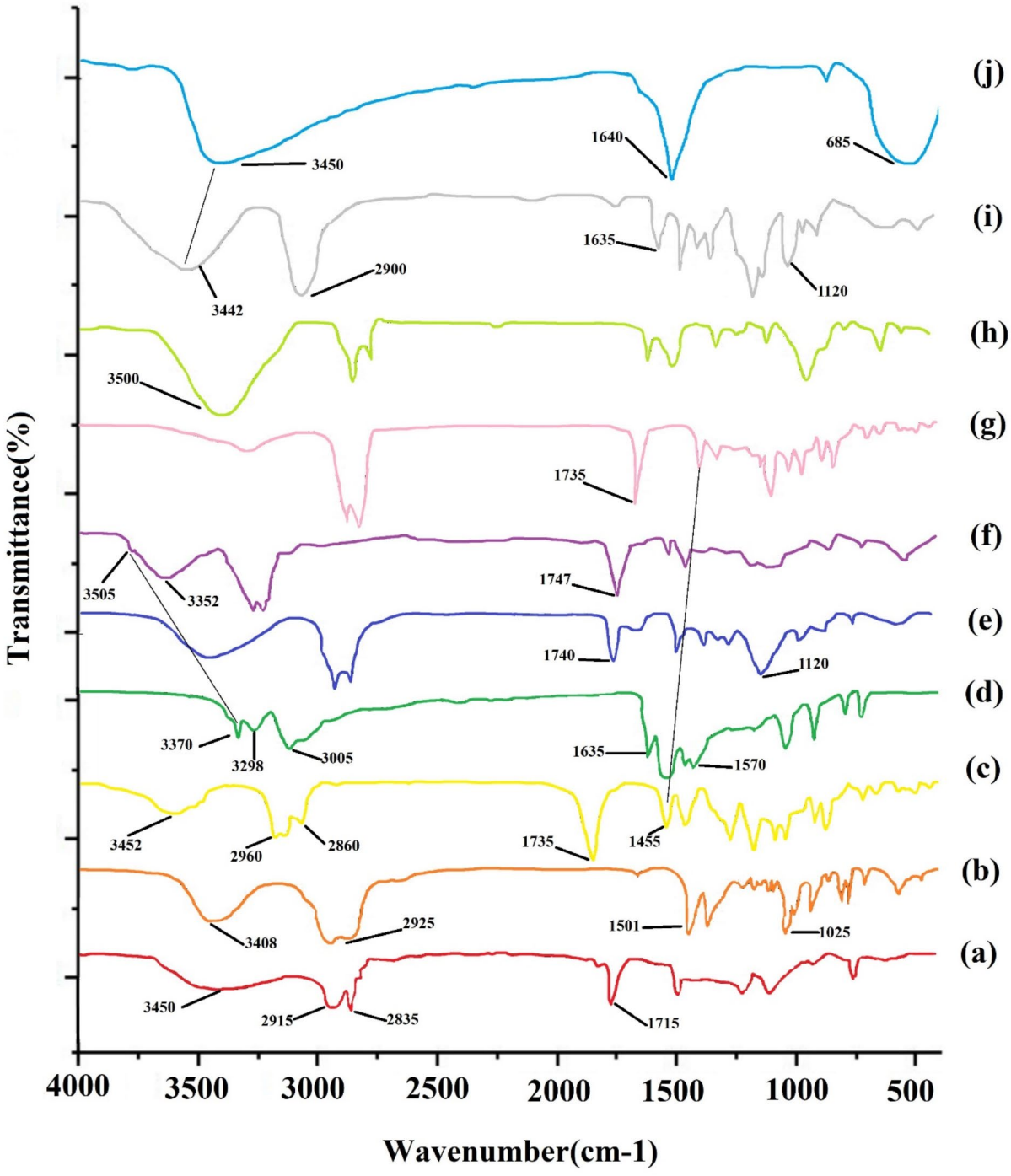

Fig. 3. FT-IR spectra of (a) span 60, (b) cholesterol, (c) ART, (d) MET, (e) Blank Nio, (f) Nio-ART-MET, (g) PNio-ART-MET, (h) PMNios-ART-MET, (i) PEG and (j) Fe_3O_4 nanoparticles.

representing C–H stretching. Additionally, a peak at 1115/cm indicated C–O stretching. The blank niosome FT-IR spectra also displayed sharp and broad peaks. The peak at 3450/cm was attributed to cholesterol and Span 60 O–H stretching, while the C–H stretch in the range of 270–2950/cm was associated with cholesterol and Span 60. The FT-IR spectrum of cholesterol exhibited a broad peak at 3408/cm, indicating O–H stretching, and peaks in the range of 2850–3050/cm, representing C–H stretching. Furthermore, a peak at 1501/cm indicated C–C stretching in the aromatic ring, and peaks in the range of 1000–1290/cm were attributed to CH_2 bending. The FT-IR spectrum of ART exhibited a broad peak at 3452/cm, indicating O–H stretching. Additionally, resonance of the CH_3 stretching was observed in the range of 2800–3000/cm, while the presence of C=O in

lactone was confirmed at 1735/cm. The O–O–C groups, which signify the 1, 2, 4-trioxane ring, were identified in the range of 1500–1300/cm. On the other hand, the FT-IR spectrum of MET displayed peaks corresponding to various functional groups. The N–H stretching was observed at 3370/cm, while the absorption of $(CH_3)_2N$ occurred in the range of 3050–2800/cm. N–H deformation was detected in the range of 1600 –700/cm, and C–N stretching was observed in the range of 1200–900/cm. Moving on to the PMNios-ART-MET, a distinct peak representing the CH_2 chain of PEG was observed, confirming the presence of PEG in the nano-niosome structure. Furthermore, the specific peaks of ART and MET were absent in the PMNios-ART-MET, indicating successful encapsulation of ART and MET by the modified niosome.

Table 1 presents the results of the measurements conducted on the prepared nano-niosomes. The zeta potential, sizes, entrapment efficiencies, and polydispersity index (PDI) of the nano-niosomes were determined and recorded. When ART and MET drugs and the magnetic Fe_3O_4 nanoparticles were added to both PEGylated-niosomes and naked niosomes, a slight increase in size was observed, while the zeta potential remained unaffected. Comparatively, the PEGylated-niosomes exhibited a slightly larger size than the naked niosomes, along with superior PDI and a slightly negative zeta potential. This negative zeta potential can be attributed to the effect of PEGylation on the niosome surface. The increase in size and decrease in zeta potential can be attributed to the presence of PEG on the niosome structure. Niosomes with a PDI value below 0.23 indicate homogeneity, greater stability, and smaller PDI, indicating more consistent samples. The presence of long chains in the PEG molecule's structure may promote the expulsion of niosomes, preventing their agglomeration and resulting in increased stability (Table 1). The difference in size measurement between SEM and DLS methods might be due to the drying process during the SEM imaging. In other words, SEM gives the size of nanoparticles in a dried form (measures exact diameter of each particle), while DLS measures the hydrodynamic diameter that includes core plus any molecule attached or adsorbed on the surface including ions and water molecules[34–36].

The stability assessment of different niosomal formulations was conducted after a storage period of 2 months at 4 ± 0.5 °C. The results confirmed that PEGylated-niosomes exhibited greater stability compared to naked niosomes. Over the course of 2 months, the size of PEGylated-niosomes only changed from 185 nm to 215 nm. Subsequently, both the PMNios-ART-MET and MNios-ART-MET were evaluated using SEM and TEM, revealing excellent size distribution and spherical morphology for both formulations. However, the PMNios-ART-MET exhibited a coarser size (Fig. 4a, b) with relatively higher dispersity and spherical shape compared to MNios-ART-MET. The average size of niosomes determined through AFM images was consistent with the size calculated through DLS analysis (Fig. 4c). It is worth noting that the AFM analysis provided a more precise measurement due to the smaller size of the dried niosomes prior to analysis. These findings align well with the results obtained from the DLS analysis (Fig. 4d). The stability studies indicated that PMNios maintained their physicochemical properties, including particle size, polydispersity index (PDI), and zeta potential, more effectively at 4 °C compared to 25 °C. This stability is crucial for ensuring consistent drug delivery and therapeutic efficacy. The PEGylation and incorporation of magnetic nanoparticles contributed to the stability by preventing aggregation and degradation. The stable physicochemical properties of PMNios enhance their suitability for clinical applications, providing a robust platform for the co-delivery of hydrophilic and hydrophobic drugs.

Evaluation of the in-vitro release of ART-MET-loaded PMNios

The subsequent step involves the assessment of the rates at which MET and ART are released from different niosomal formulations (Table 1). Based on the drug release pattern, both the PMNios and PNios (without magnetic nanoparticles) formulations exhibit a bi-phasic pattern, as depicted in Fig. 5. It is evident that all patterns display an initial rapid-release phase, with approximately 40% of the drugs being released within the first 20 h. Subsequently, a more stable and slower release occurs over the next 52 h. Furthermore, the presence of magnetic nanoparticles leads to a reduction in the drug release from various niosomal formulations. It is worth noting that the PEGylation of all niosomal formulations, which encapsulate both magnetic nanoparticles and drugs, results in a slower release compared to PNios formulations. This finding aligns with our previous research, highlighting the effectiveness of PEGylation in enhancing the drug release kinetics from magnetic nano-niosome structures[27]. The release kinetics of different formulations were studied using different kinetic models (Table 2). The value of R2 determines the best model for each formulation. The sample with the highest value of R2 was chosen as a suitable model for the release mechanism.

In-vitro effect of the modified noisome formulations on A549 lung cancer cell and HBE normal cell

The effect of the synthesized ART- and MET-loaded nano-niosome formulations was investigated in vitro toward A549 cell line, a well-evaluated lung cancerous cell line, and human epithelial (HBE) cell by MTT assay. ART is an anti-cancer phytochemical that is used against lung cancer, hepatocellular carcinoma, breast cancer, carcinoma and colorectal cancer. On the other hand, MET has the efficiency to reduce the growth of various cancer like lung, colorectal, hepatic carcinoma and breast cancers. The results of treatment of A549 cancer cell line and HBE cell line with free drugs and various modified niosomes at concentrations, 3.863, 134, 17.92 and 12.55 µg/mL for free MET, free ART, Nios-ART-MET and PMNios-ART-MET, respectively for 48 h show in Figs. 6 and 7. The data from the charts indicate that the empty niosomes did not have any significant effects. However, when ART and MET were loaded into PEGylated niosomes, the drugs had a noticeably increased effect. Furthermore, we evaluated the impact of an external magnetized field on the viability of A549 cancer cells. The influence of an external neodymium magnet with a magnetic field of 1.3 T on the niosome uptake and treatment impact was evaluated by using an external magnet under the 96-well plate for 15 min under the 96-well plate 48-h incubation Fig. 8. The application of this external field on the modified magnetic-niosome (PMNios-ART-MET + external magnetic field) resulted in a decrease in viability to 45%, compared to a 60% reduction in viability observed in the PMNios-ART-MET without the external magnetic field ($p < 0.001$). Taking these findings into consideration,

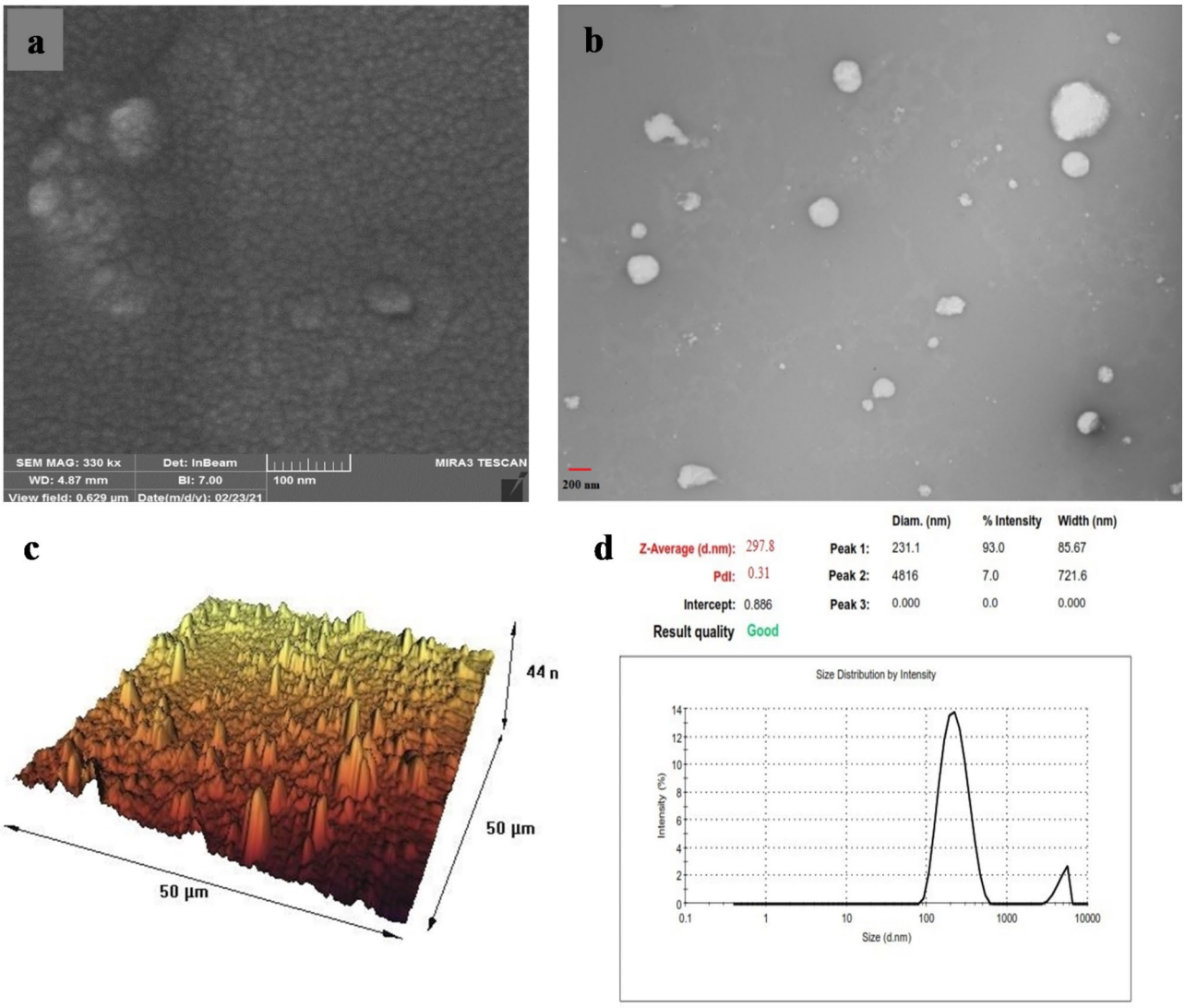

Fig. 4. (a) The field emission scanning electron microscopy; (b) the transmission electron microscopy of the prepared PMNios-ART-MET; (c) microscopic images using atomic force microscopy of the PMNios-ART-MET; (d) size distribution by intensity.

it can be concluded that the PMNios-ART-MET, when combined with an external magnetic field, exhibits sufficient toxicity against the targeted cancerous cell line. According to Fig. 7 none of the free ART, free MET and niosomal formulations have considerable cytotoxicity on HBE normal cell lines. Our results demonstrated that artemisinin concentration-induced cytotoxicity in cancer cells is more obvious and has minimal cytotoxicity in normal cells. Also, metformin concentration-induced cytotoxicity in cancer cells is more but has very minor cytotoxicity in normal cells. PEGylated magnetic niosome with encapsulated ART and MET has no cytotoxicity on normal cells but has an impressive effect on cancer cells. Our study offers that the cytotoxic effect of MET and ART and their niosomal formulation deserve more study before ART and MET are utilized in clinical treatments. As shown in Table 3, the IC50 values of all formulations were compared. Next, the combination index (CI) was calculated in 48 h using the Chou-Talalay method (Table 4). The synergistic combination of ART and MET within PEGylated magnetic nanoniosomes leverages multiple molecular mechanisms to exert potent anticancer effects. These mechanisms include apoptosis induction, and AMPK activation along with enhanced targeted delivery and cellular uptake. This multi-faceted approach holds promise for improving chemotherapeutic efficacy and reducing adverse effects in cancer therapy. The observed differences in cell viability between the PEGylated magnetic nanoniosomes (PMNios-drug) and the non-PEGylated niosomes (Nios-drug) across different drugs can be attributed to the distinct physicochemical properties and delivery efficiencies imparted by PEGylation and magnetic components. For metformin (MET), the higher cell viability in the PMNios-MET group compared to the Nios-MET group is likely due to a slower release rate and altered intracellular distribution, resulting in reduced immediate cytotoxic effects. Conversely, for artemisinin (ART), the PEGylation and magnetic targeting enhance drug stability, solubility, and uptake, leading to more effective ROS generation and apoptosis induction, thereby lowering cell viability in the PMNios-ART group compared to the Nios-ART group. These findings

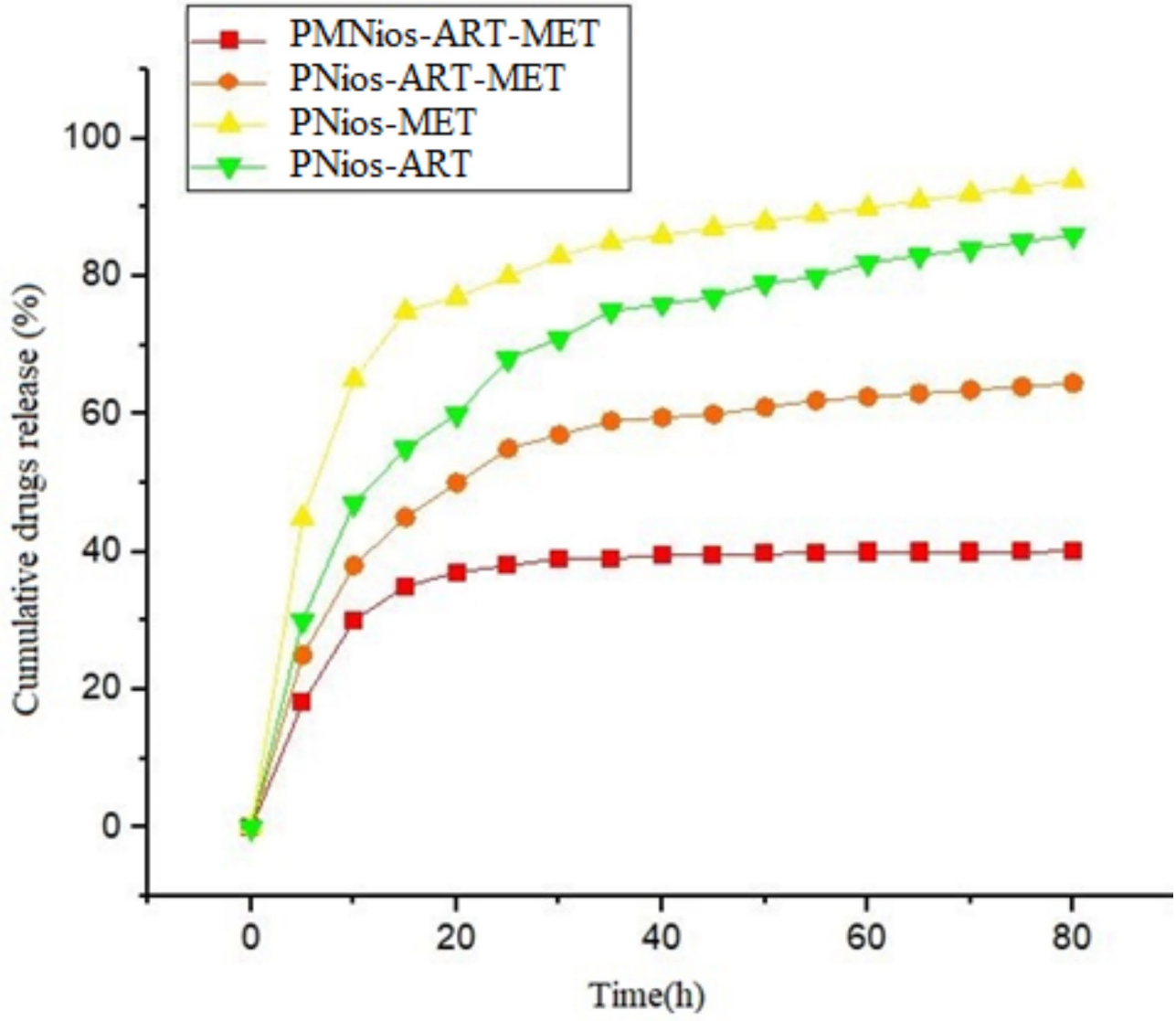

Fig. 5. In vitro drugs release of the PNios-ART, PNios-MET, PNios-ART-MET and PMNios-ART-MET.

Kinetic Model		Zero-Order $C_t=C_0+K_0t$ r^2	First-Order $LogC=LogC0+K_t/2.303$ r^2	Higuchi $Q=K_H\sqrt{t}$ r^2	Korsmeyer-Peppas $M_t/M=K_t.t^n$ r^2	n^*
ART	pH 7.4	0.8034	0.9435	0.9124	0.9393	0.3439
MET	pH 7.4	0.7163	0.9453	0.8377	0.8868	0.2204
ART-MET-PEG-N	pH 7.4	0.7189	0.7982	0.8483	0.9007	0.3031
ART-MET-PEG-NPs-N	pH 7.4	0.4679	0.4975	0.6156	0.7188	0.2182

Table 2. The kinetic release models and the parameters. * Diffusion or release exponent.

highlight the importance of nanoparticle formulation and targeting strategies in modulating drug delivery and therapeutic outcomes. The PEGylation and incorporation of magnetic nanoparticles enhance the stability and systemic circulation time of the nanoniosomes. For metformin (MET), this can result in a slower release rate from PMNios compared to Nios. Consequently, the immediate bioavailability of MET might be reduced in the PMNios formulation, leading to higher cell viability in short-term assays. The magnetic component might also influence the uptake kinetics and intracellular distribution of MET, potentially reducing its immediate cytotoxic effects compared to the non-PEGylated version. In contrast, artemisinin (ART) benefits significantly from the

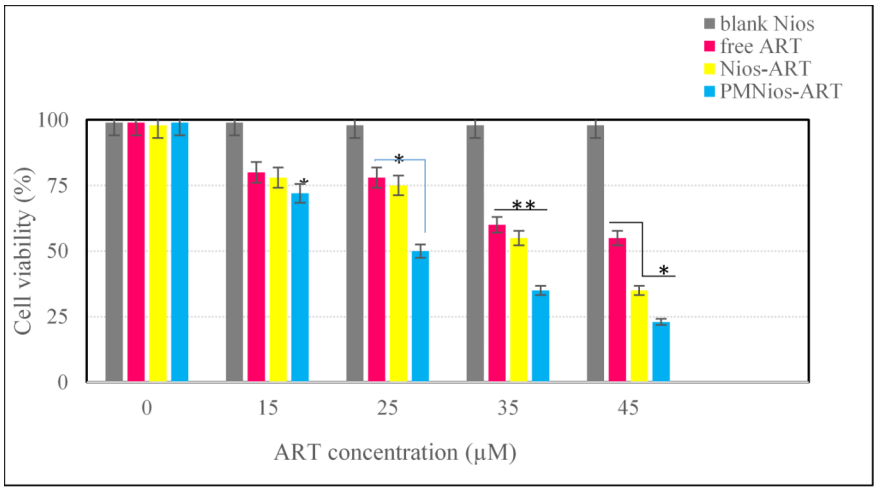

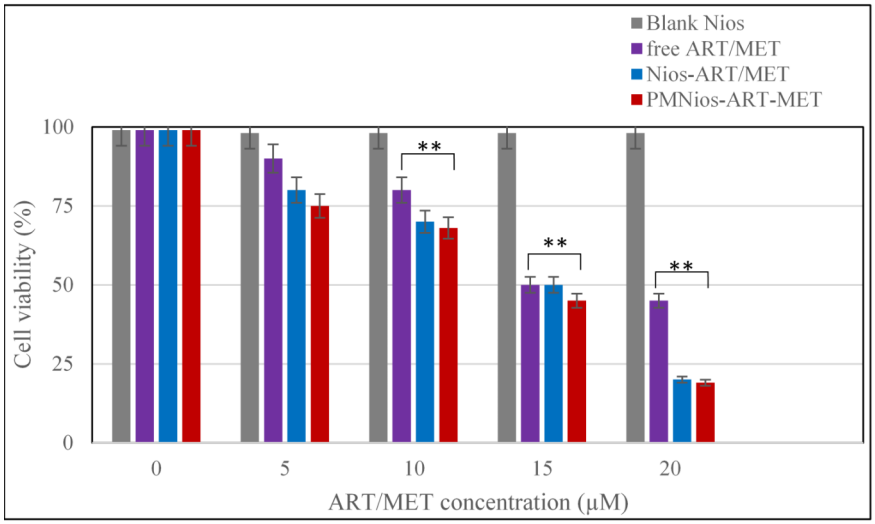

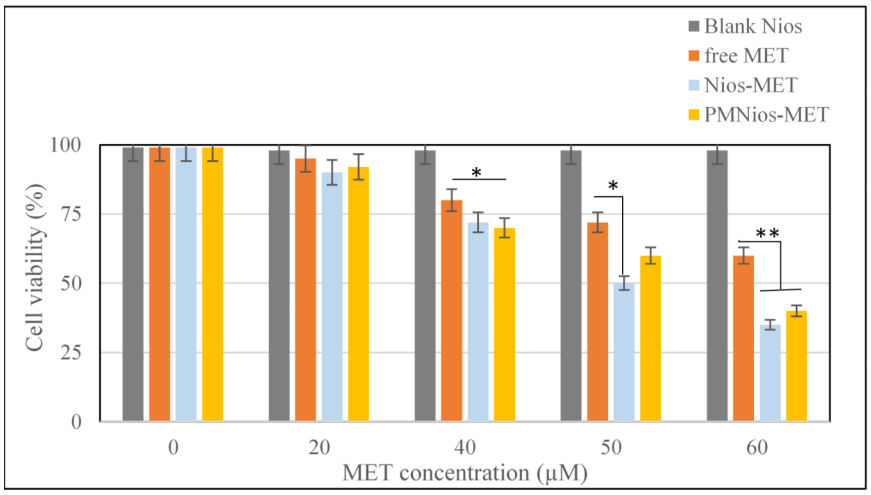

Fig. 6. Cell viability of A549 lung cancer cells and control after treatment with various concentrations of free ART, free MET, free ART/MET, Nio-ART, Nio-MET, Nio-ART/MET, PNios-ART-MET and PMNios-ART-MET after 48 h against A549 cells. Free ART/MET and niosomal ART/MET and PEGylated niosomal ART-MET have no cytotoxicity. Data are shown as Mean ± SD, $n = 3$ (* $P < 0.05$, ** $P < 0.01$ and *** $p < 0.001$).

targeted delivery and enhanced cellular uptake provided by PEGylation and magnetic guidance. The magnetic targeting ensures a higher concentration of ART is delivered directly to the cancer cells, increasing its cytotoxic efficiency. Additionally, the PEGylation can facilitate better penetration and sustained release of ART within the tumor microenvironment, leading to more effective ROS generation and apoptosis induction, thereby reducing

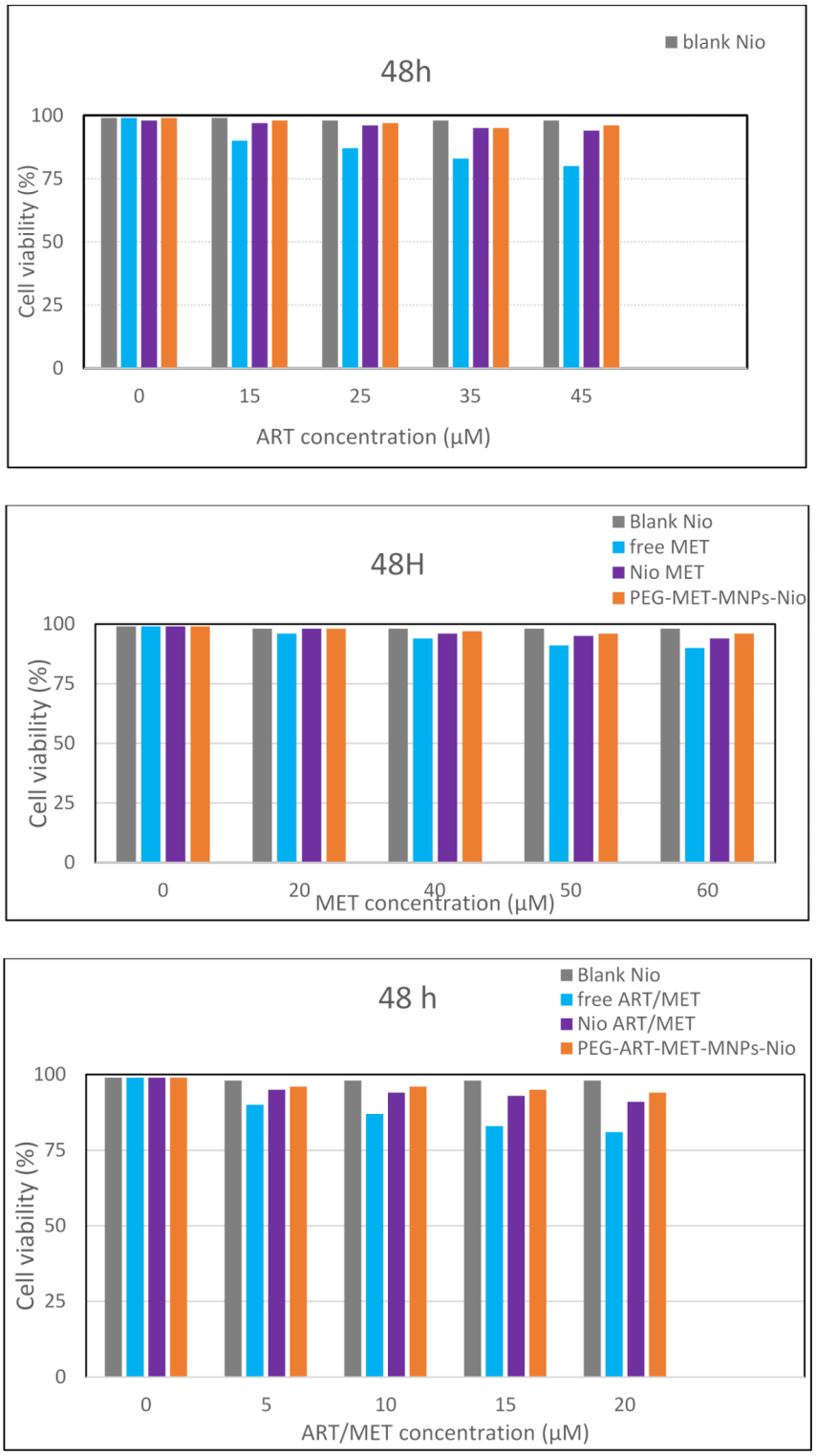

Fig. 7. Cell viability of HBE cells and control after treatment with various concentrations of free ART, free MET, free ART/MET, Nio-ART, Nio-MET, Nio-ART/MET, PNios-ART-MET and PMNios-ART-MET after 48 h against HBE cells. Free ART/MET and niosomal ART/MET and PEGylated niosomal ART-MET have no considerable cytotoxicity. Data are shown as Mean ± SD, $n = 3$ (* $P < 0.05$, ** $P < 0.01$ and *** $p < 0.001$).

cell viability more effectively than the non-PEGylated formulation[37]. The encapsulation of drugs in PEGylated magnetic nanoniosomes can alter their release profiles. For MET, a hydrophilic drug, the encapsulation within PMNios might slow its release, leading to a delayed cytotoxic effect compared to Nios. This delayed release can result in higher cell viability in initial observations[38]. For ART, a hydrophobic drug, PEGylation and magnetic

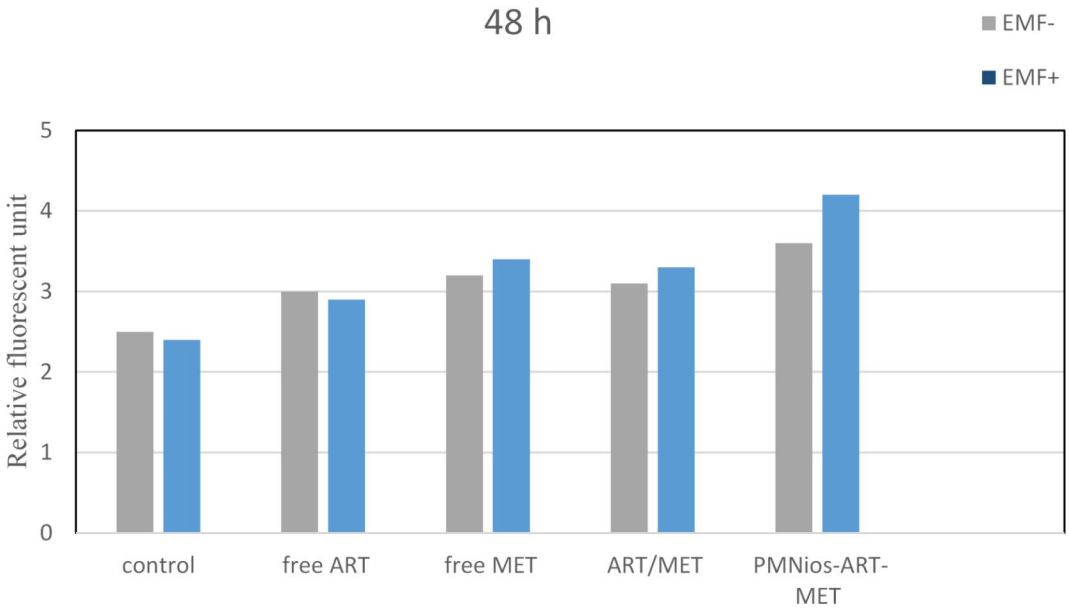

Fig. 8. Apoptotic effect with or without the presence of an external magnetic field in the various niosomal formulations (all data showing $p < 0.05$ considered significant). EMF-: no external magnetic field, EMF+: presence of an external magnetic field.

Concentrations (µM)	
Free MET	68.33333
Nio MET	50
PEG-MET-MNPs-Nio	55
Free ART	70
Nio ART	52.5
PEG-ART-MNPs-Nio	40
Free ART/MET	50
Nio ART/MET	50
PEG-ART-MET-MNPs-Nio	47.82609

Table 3. IC50 value of formulations.

CI Factor				
Concentrations (µM)	**20**	**40**	**50**	**60**
Free MET & Free ART	1.1379	1.3482	0.723	0.7717
Nio MET & Nio ART	0.8057	1.2119	0.9762	0.5837
PEG-MET-MNPs-Nio & PEG-ART-MNPs-Nio	0.7371	1.2457	0.9797	0.645

Table 4. Combination index (CI) for formulations.

targeting can enhance its solubility, stability, and cellular uptake, facilitating a more rapid and sustained release at the target site, thus exerting a more potent cytotoxic effect and reducing cell viability more effectively. Also, the magnetic component in PMNios can enhance the accumulation of the drug-loaded nanoparticles at the tumor site under an external magnetic field, improving the uptake of ART. The increased intracellular concentration of ART leads to higher ROS production and apoptosis, reducing cell viability. In the case of MET, the magnetic targeting might influence its distribution and intracellular trafficking, potentially reducing its immediate availability to exert its cytotoxic effects, thereby resulting in higher cell viability in the PMNios-MET group compared to the Nios-MET group.

Gene expression by RT-PCR

The molecular evaluation of the anticancer properties of ART and MET encapsulated in PEGylated niosome involved assessing the expression of apoptotic genes *Bcl2* and *Bax* using the real-time PCR technique. A549 lung

cancer cells were treated with IC50s of various niosomal and free forms of ART and MET after 72 h of incubation (Fig. 8). The *Bax* and *Bcl2* genes, which belong to the cysteine protease group and are responsible for controlling mitochondria-mediated apoptosis, were analyzed. It was expected that changes in their expression rates would enhance apoptosis and inhibit the growth of lung cancer cells. The results of the surveys showed that treatment with different niosomal formulations of ART and MET led to a significant upregulation of the *Bax* gene and down-regulation of the *Bcl2*gene in the cancer cells compared to free ART and MET. The most notable expression rates of these genes were observed in the cells treated with Nios-ART-MET. This outcome indicates that the co-delivery of ART and MET has a significant impact on inducing apoptosis in A549 lung cancer cell lines, which is consistent with the MTT results. Therefore, this study demonstrates that the simultaneous release of these two anticancer drugs through magnetic niosomes results in pro-apoptotic effects and synergistic cytotoxicity against A549 lung cancer cells. The genes *Bax* and *Bcl2* play critical roles in the regulation of apoptosis, a key mechanism in cancer treatment. Their expression levels and interactions can significantly influence the effectiveness of anticancer therapies. *Bax* is a pro-apoptotic protein that promotes cell death by facilitating the release of cytochrome c from mitochondria into the cytosol, a crucial step in the intrinsic pathway of apoptosis. Upregulation of *Bax* enhances the sensitivity of cancer cells to chemotherapeutic agents by promoting apoptosis. *Bcl2* is an anti-apoptotic protein that prevents apoptosis by inhibiting the release of cytochrome c from the mitochondria. *Bcl2* binds to pro-apoptotic proteins like *Bax* and Bak, sequestering them and preventing their activation and oligomerization on the mitochondrial membrane. Overexpression of *Bcl2* is a common feature in many cancers, contributing to resistance against chemotherapy and radiation therapy by inhibiting apoptosis. Therapeutic strategies often aim to downregulate *Bcl2* or block its function to restore the apoptotic capability of cancer cells. The ratio of *Bax* to *Bcl2* is a critical determinant of cell fate. A higher *Bax*/ *Bcl2* ratio favors apoptosis, making cancer cells more prone to die in response to therapy. Conversely, a lower ratio indicates resistance to apoptosis and is often associated with poor therapeutic outcomes[39–43] (Fig. 9).

Cell uptake

Confocal microscopy images (Fig. 10) demonstrated the cellular uptake of FITC-labeled PMNios formulations (PMNios-MET, PMNios-ART, and PMNios-ART-MET) by A549 cells over time. Control samples stained solely with DAPI exhibited nuclear staining without FITC fluorescence.

These results reveal significant insights into the cellular uptake and distribution of PEGylated magnetic nano-niosomes (PMNios) loaded with metformin (MET) and artemisinin (ART). In the control samples, where only DAPI dye was used, the fluorescence was limited to the cell nuclei, and no fluorescence from FITC was observed, indicating no nanoparticle penetration. The DAPI fluorescence intensity remained constant from 1 to 8 h, suggesting stable dye retention in the nuclei. In contrast, the PMNios-MET and PMNios-ART nanoparticles demonstrated substantial cellular penetration, with the fluorescence intensity peaking at 8 h, indicating maximum nanoparticle uptake. This observation aligns with previous studies where niosomes have shown efficient drug delivery and cellular uptake due to their favorable size and surface properties[8,10]. Notably, the PMNios-ART-MET nanoparticles exhibited even higher penetration into the cytoplasm, achieving the

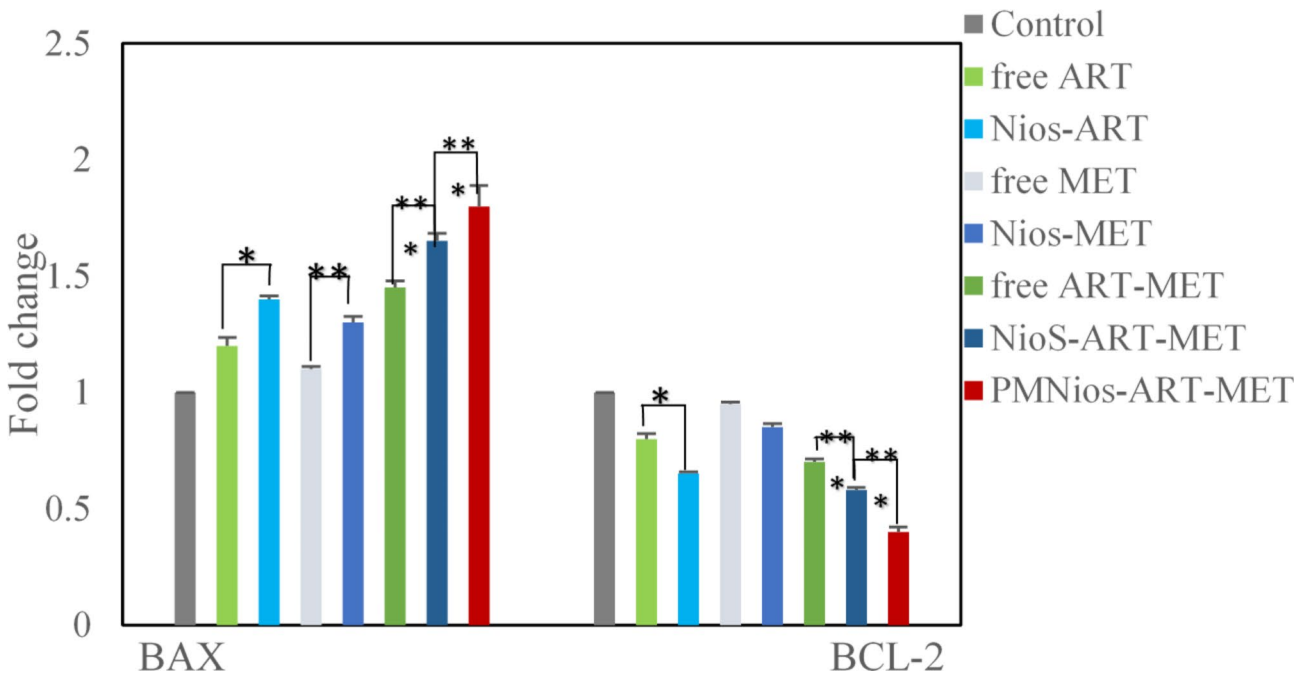

Fig. 9. The expression rate of *Bcl2* and *Bax* in A549 lung cancer cells treated with free ART, Nios-ART, free MET, Nios-MET, free ART-MET, Nios-ART-MET and PMNios-ART-MET after 72 h incubation time. (***$p < 0.001$, **$p < 0.01$, and *$p < 0.05$). Results are mean ± SD ($n = 3$).

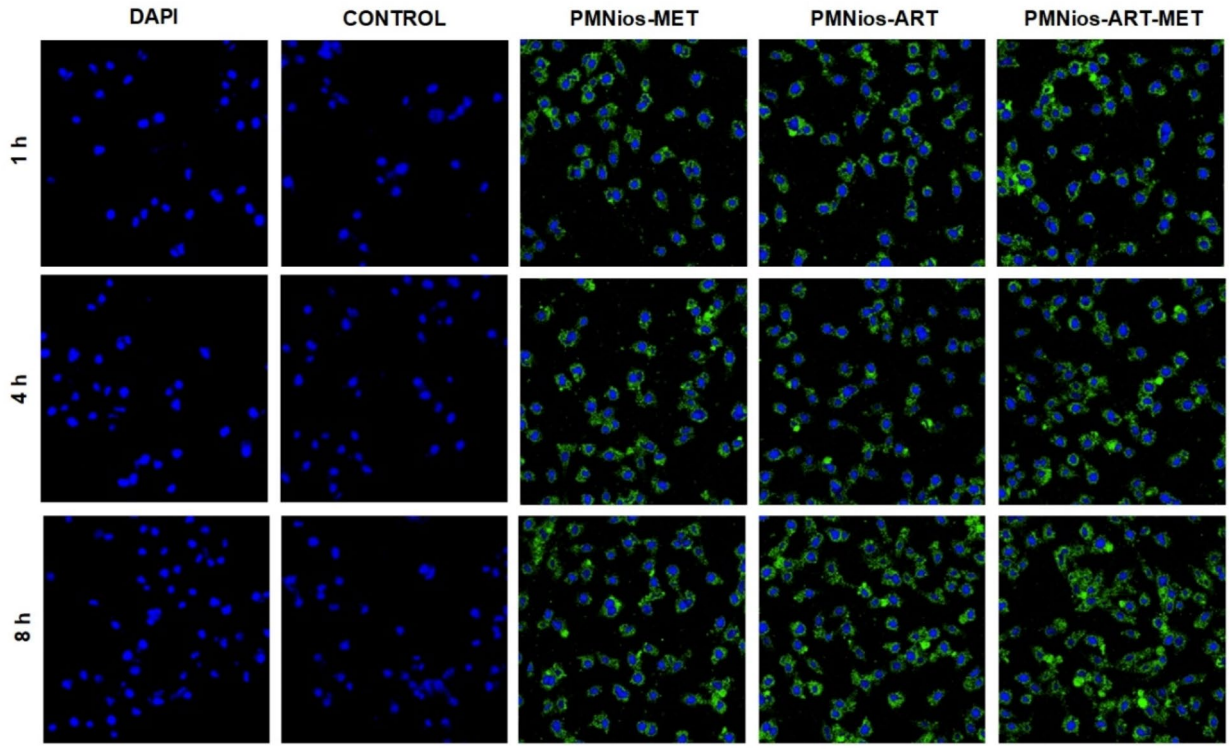

Fig. 10. Cellular Uptake of FITC-Labeled Nanoparticles in A549 Cells. Confocal microscopy images showing the uptake of FITC-labeled nanoparticles (PMNios-MET, PMNios-ART, and PMNios-ART-MET) at a concentration of 15 μM by A549 cells after 1, 4, and 8 h of incubation.

highest fluorescence intensity after 8 h. This enhanced penetration can be attributed to the synergistic effects of MET and ART, which have been shown to improve the therapeutic efficacy and cellular uptake of drug-loaded nanoparticles[44]. The increased cytoplasmic localization of PMNios-ART-MET suggests a more effective delivery mechanism, potentially leading to better therapeutic outcomes. This is consistent with findings that niosomes can co-deliver multiple drugs, enhancing their cytotoxic effects and overcoming drug resistance[8,45]. Additionally, the stability and slow-release properties of niosomes, as demonstrated in other studies, likely contribute to the sustained fluorescence observed over the 8-hour period[45,46]. Overall, the confocal microscopy results underscore the potential of PMNios-ART-MET as a superior drug delivery system, capable of achieving higher intracellular concentrations and improved therapeutic efficacy.

Bioavailability of artemisinin and metformin in niosomal formulation

Niosome novel drug delivery system has improved as an effective technique to dominate some limited due to their benefits like high stability, low cost, biodegradability, flexibility and high stability to encapsulate hydrophilic and lipophilic drugs. According to our study, the bioavailability of ART and MET has been effectively increased by utilizing a modified niosome drug delivery system. Based on this information, it can be proven that niosome has improved significance in bioavailability increase and upgrade the total efficiency of ART and MET drugs in-vivo and in-vitro. Therefore, niosome drug delivery system has a more efficient potential for scale-up usage, overcoming the dose-dependent of various drugs.

Conclusions

In summary, we have made modifications to nano-carrier by incorporating magnetic Fe_3O_4 nanoparticles and encapsulating them within a niosome structure. This innovative approach allows us to trap both hydrophobic ART and hydrophilic MET drugs within the modified niosomal nano-carrier and assess its potential for treating lung cancer. The results indicate that the modified nano-carriers exhibited excellent biocompatibility with normal cells. Furthermore, this modified nano-carrier demonstrated significant cytotoxicity against the tested lung cancer cell line (A549). The findings suggest that the co-delivery of ART and MET resulted in increased apoptosis in A549 cancer cells, which can be attributed to the regulation of gene expression in these cells. Additionally, the evaluation of cell migration revealed that the co-delivery of ART and MET by the PMNios potentially reduces the migration rate of lung cancer cells, thereby impeding their spread within the body and delaying metastasis. The incorporation of ART and MET into PEGylated magnetic niosome resulted in reduced drug toxicity, improved cellular uptake, improved drug solubility and regulated release of the drugs resulting in

improved bioavailability. Overall, the modified niosomes exhibit great potential for effective chemotherapy in lung cancer cells. The outcomes of our study may pave the way for novel approaches in nanomedicine research and provide new insights to the scientific community for the design of targeted nano-carriers in future cancer therapy. In this study, we entrapped ART and MET in PEGylated magnetic niosome nano-vesicles. In-vitro studies have proven the selective cytotoxicity of A549 cancer cells. Future pre-clinical and in-vivo investigations will be investigated in the next project.

Data availability

The data that support the findings of this study are available from the corresponding author upon reasonable request.

Received: 26 April 2024; Accepted: 4 November 2024
Published online: 09 November 2024

References

1. Witika, B. A., Bassey, K. E., Demana, P. H., Siwe-Noundou, X. & Poka, M. S. Investigating the use of niosomes in pharmaceuticals and drug delivery. *Int. J. Pharm. Res. Allied Sci.* **13**, 85 (2024).
2. Sharma, S., Garg, A., Agrawal, R., Chopra, H. & Pathak, D. A comprehensive review on niosomes as a tool for advanced drug delivery. *Pharm. Nanatechnol.* **12**, 206–228 (2024).
3. Javan, E. S. et al. Development of a magnetic nanostructure for co-delivery of metformin and silibinin on growth of lung cancer cells: possible action through leptin gene and its receptor regulation. *Asian Pac. J. Cancer Prevent.: APJCP* **23**, 519 (2022).
4. Javaid, S., Rana, T., Naeem, Z. & Sajid, N. Exploring niosomes: a comprehensive review of their structure, formulation, and biomedical applications. *Currents Pharm. Res.* **2**, 01–34 (2024).
5. Shafiei, G. et al. Targeted delivery of silibinin via magnetic niosomal nanoparticles: potential application in treatment of colon cancer cells. *Front. Pharmacol.* **14**, 147 (2023).
6. Abdulkareem, S. J. et al. Co-delivery of artemisinin and metformin via PEGylated niosomal nanoparticles: potential anti-cancer effect in treatment of lung cancer cells. *DARU J. Pharm. Sci.* **32**, 133–144 (2024).
7. Al-Kofahi, T. et al. Paclitaxel-loaded niosomes in combination with metformin: development, characterization and anticancer potentials. *Therapeutic Deliv.* **15**, 109–118 (2024).
8. Sharifi-Azad, M. et al. Codelivery of methotrexate and silibinin by niosome nanoparticles for enhanced chemotherapy of CT26 colon cancer cells. *Biomed. Mater.* **19**, 055015 (2024).
9. Kaur, D. & Kumar, S. Niosomes: present scenario and future aspects. *J. Drug Deliv. Ther.* **8**, 35–43 (2018).
10. Riazi, H., Goodarzi, M. T., Tabrizi, M. H., Mozaffari, M. & Neamati, A. Preparation of the myricetin-loaded PEGylated niosomes and evaluation of their in vitro anti-cancer potentials. *Chem. Biodivers.* **21**, e202301767 (2024).
11. Tariq, F. et al. Optimization & characterization of niosomal & polymeric nanoparticles. *Int. J. Polym. Mater. Polym. Biomaterials* **73**, 1353–1366 (2024).
12. Osman, N. et al. Niosomes modified with a novel pH-responsive coating (mPEG-OA) enhance the antibacterial and anti-biofilm activity of Vancomycin against methicillin-resistant *Staphylococcus aureus*. *Nano Express* **5**, 015008 (2024).
13. Hassani, N., Jafari-Gharabaghlou, D., Dadashpour, M. & Zarghami, N. The effect of dual bioactive compounds artemisinin and metformin co-loaded in PLGA-PEG nano-particles on breast cancer cell lines: potential apoptotic and anti-proliferative action. *Appl. Biochem. Biotechnol.* **194**, 4930–4945 (2022).
14. Abdelaziz, A. A., Elbanna, T. E., Sonbol, F. I., Gamaleldin, N. M. & El Maghraby, G. M. Optimization of niosomes for enhanced antibacterial activity and reduced bacterial resistance: in vitro and in vivo evaluation. *Expert Opin. Drug Deliv.* **12**, 163–180 (2015).
15. Balakrishnan, P. et al. Formulation and in vitro assessment of minoxidil niosomes for enhanced skin delivery. *Int. J. Pharm.* **377**, 1–8 (2009).
16. Barani, M. et al. In silico and in vitro study of magnetic niosomes for gene delivery: the effect of ergosterol and cholesterol. *Mater. Sci. Eng. C* **94**, 234–246 (2019).
17. Huang, Y., Chen, J., Chen, X., Gao, J. & Liang, W. PEGylated synthetic surfactant vesicles (Niosomes): novel carriers for oligonucleotides. *J. Mater. Science: Mater. Med.* **19**, 607–614 (2008).
18. Firouzi Amandi, A. et al. Fabrication of magnetic niosomal platform for delivery of resveratrol: potential anticancer activity against human pancreatic cancer Capan-1 cell. *Cancer Cell Int.* **24**, 46 (2024).
19. Masoumi Godgaz, S., Asefnejad, A. & Bahrami, S. H. Fabrication of PEGylated SPIONs-loaded niosome for codelivery of paclitaxel and trastuzumab for breast cancer treatment: in vivo study. *ACS Appl. Bio Mater.* **7**, 2951–2965 (2024).
20. Ibrahim, N. et al. Artemisinin nanoformulation suitable for intravenous injection: preparation, characterization and antimalarial activities. *Int. J. Pharm.* **495**, 671–679 (2015).
21. Want, M. Y. et al. A new approach for the delivery of artemisinin: formulation, characterization, and ex-vivo antileishmanial studies. *J. Colloid Interface Sci.* **432**, 258–269 (2014).
22. Asgharkhani, E., Najmafshar, A. & Chiani, M. Artemisinin (ART) drug delivery using mixed non-ionic surfactants and evaluation of their efficiency in different cancer cell lines. *Int. J. Drug Deliv. Technol.* **4**, 67–71 (2014).
23. Asgharkhani, E. et al. Artemisinin-loaded niosome and pegylated niosome: physico-chemical characterization and effects on MCF-7 cell proliferation. *J. Pharm. Invest.* **48**, 251–256 (2018).
24. Emami, J., Yousefian, H. & Sadeghi, H. Targeted nanostructured lipid carrier for brain delivery of artemisinin: design, preparation, characterization, optimization and cell toxicity. *J. Pharm. Pharm. Sci.* **21**, 225s–241s (2018).
25. Parekh, F., Patel, B., Vyas, K. & Patani, P. Recent advances and scopes in niosomes. *J. Pharm. Negat. Results* **2022**, 2093–2102 (2022).
26. Witika, B. A., Bassey, K. E., Demana, P. H., Siwe-Noundou, X. & Poka, M. S. Current advances in specialised niosomal drug delivery: manufacture, characterization and drug delivery applications. *Int. J. Mol. Sci.* **23**, 9668 (2022).
27. Shahbazi, R., Jafari-Gharabaghlou, D., Mirjafary, Z., Saeidian, H. & Zarghami, N. Design and optimization various formulations of PEGylated niosomal nanoparticles loaded with phytochemical agents: potential anti-cancer effects against human lung cancer cells. *Pharmacol. Rep.* **75**, 442–455 (2023).
28. Davarpanah, F., Khalili Yazdi, A., Barani, M., Mirzaei, M. & Torkzadeh-Mahani, M. Magnetic delivery of antitumor carboplatin by using PEGylated-Niosomes. *DARU J. Pharm. Sci.* **26**, 57–64 (2018).
29. Babatabar, M. A. et al. Production of mid-distillation fuels from syngas using cobalt nanocatalyst supported on Gracilaria gracilis macroalgae biochar. *J. Farayandno–Vol* **17**, 38–53 (2022).
30. Babatabar, M. A., Manouchehri, M., Abbasi, H. & Tavasoli, A. Supercritical water co-gasification of biomass and plastic wastes for hydrogen-rich gas production using Ni-Cu/AC-CaO catalyst. *J. Energy Inst.* **108**, 101251 (2023).
31. Khallaf, R. A., Aboud, H. M. & Sayed, O. M. Surface modified niosomes of olanzapine for brain targeting via nasal route; preparation, optimization, and in vivo evaluation. *J. Liposome Res.* **30**, 163–173 (2020).

32. Singh, N. P. & Lai, H. C. Synergistic cytotoxicity of artemisinin and sodium butyrate on human cancer cells. *Anticancer Res.* **25**, 4325–4331 (2005).
33. He, R. X. et al. PEGylated niosomes-mediated drug delivery systems for Paeonol: preparation, pharmacokinetics studies and synergistic anti-tumor effects with 5-FU. *J. Liposome Res.* **27**, 161–170 (2017).
34. Ghafelehbashi, R. et al. Preparation, physicochemical properties, in vitro evaluation and release behavior of cephalexin-loaded niosomes. *Int. J. Pharm.* **569**, 118580 (2019).
35. Akbarzadeh, I. et al. Niosomal delivery of simvastatin to MDA-MB-231 cancer cells. *Drug Dev. Ind. Pharm.* **46**, 1535–1549 (2020).
36. Pashizeh, F. et al. Bioresponsive gingerol-loaded alginate-coated niosomal nanoparticles for targeting intracellular bacteria and cancer cells. *Int. J. Biol. Macromol.* **258**, 128957 (2024).
37. Mohapatra, P., Singh, D. & Sahoo, S. K. PEGylated nanoparticles as a versatile drug delivery system. *Nanoeng. Biomater.* **2022**, 309–341 (2022).
38. Banerjee, D. & Bose, S. Comparative effects of controlled release of sodium bicarbonate and doxorubicin on osteoblast and osteosarcoma cell viability. *Mater. Today Chem.* **12**, 200–208 (2019).
39. Ola, M. S., Nawaz, M. & Ahsan, H. Role of Bcl-2 family proteins and caspases in the regulation of apoptosis. *Mol. Cell. Biochem.* **351**, 41–58 (2011).
40. Burlacu, A. Regulation of apoptosis by Bcl-2 family proteins. *J. Cell. Mol. Med.* **7**, 249–257 (2003).
41. Thomadaki, H. & Scorilas, A. BCL2 family of apoptosis-related genes: functions and clinical implications in cancer. *Crit. Rev. Clin. Lab. Sci.* **43**, 1–67 (2006).
42. Ahmadi, M. et al. Cytotoxic and apoptosis-inducing properties of Staphylococcus aureus cytoplasmic extract on lung cancer cells: insights from MTT assay and bax/bcl-2 gene expression analysis. *Gene Rep.* **2024**, 101955 (2024).
43. Tofigh, P., Mirghazanfari, S. M., Hami, Z., Nassireslami, E. & Ebrahimi, M. The investigation of Quercus Infectoria Gall Aqueous Extract Effect on the cell proliferation, apoptosis and expression of CCND1, TP53, BCL2 and BAX genes in cell line of lung, gastric and esophageal cancers. *Rep. Biochem. Mol. Biol.* **12**, 596 (2024).
44. Salmani-Javan, E., Jafari-Gharabaghlou, D., Bonabi, E. & Zarghami, N. Fabricating niosomal-PEG nanoparticles co-loaded with metformin and silibinin for effective treatment of human lung cancer cells. *Front. Oncol.* **13**, 1193708 (2023).
45. Safari Sharafshadeh, M., Tafvizi, F., Khodarahmi, P. & Ehtesham, S. Folic acid-functionalized PEGylated niosomes co-encapsulated cisplatin and doxoribicin exhibit enhanced anticancer efficacy. *Cancer Nanotechnol.* **15**, 14 (2024).
46. Moghadam, Z. S. M., Mansour, F. N., Naseroleslami, M. & Niri, N. M. Preparation, characterization, and evaluation of the antimicrobial effects of farnesol-and tyrosol-bearing nanoniosomes on *Pseudomonas aeruginosa, Staphylococcus aureus*, and *Escherichia coli*. *Med. J. Tabriz Univ. Med. Sci.* (2024).

Acknowledgements

The authors would like to acknowledge the Tabriz University of Medical Sciences and Islamic Azad University Science and Research Branch for providing the necessary laboratory facilities for this study.

Author contributions

R.S. designed the experiments and wrote the manuscript. N.Z., Z.M. and H.S analyzed the data and edited the manuscript. All authors confirmed the final manuscript before submission. All authors have read and agreed to the published version of the manuscript.

Funding

Not applicable.

Competing interests

The authors declare no competing interests.

Ethical approval

The authors have fully observed the ethical points in conducting the research and writing the results. All methods were carried out in accordance with relevant guidelines and regulations. All experimental protocols were approved by the Islamic Azad University Research Committee. Informed consent was obtained from all subjects and/or their legal guardian(s).

Additional information

Correspondence and requests for materials should be addressed to Z.M. or N.Z.